Article

Dynamic Dielectric Response of Concentrated Colloidal Dispersions: Comparison between Theory and Experiment

B. H. Bradshaw-Hajek, S. J. Miklavcic, and L. R. White

Langmuir, **2009**, 25 (4), 1961-1969• DOI: 10.1021/la8028963 • Publication Date (Web): 20 January 2009

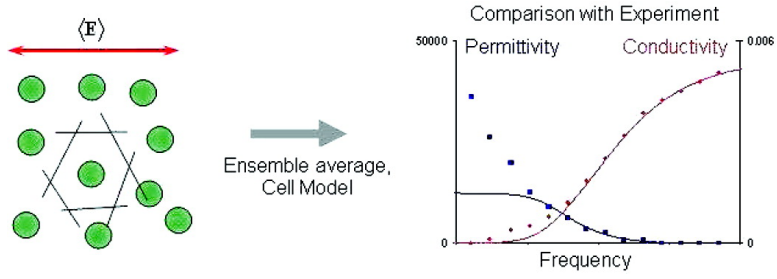

More About This Article

Additional resources and features associated with this article are available within the HTML version:

- Supporting Information
- Access to high resolution figures
- Links to articles and content related to this article
- Copyright permission to reproduce figures and/or text from this article

View the Full Text HTML

Dynamic Dielectric Response of Concentrated Colloidal Dispersions: Comparison between Theory and Experiment†

B. H. Bradshaw-Hajek,*,‡,§ S. J. Miklavcic,‡ and L. R. White‡

School of Mathematics and Statistics, University of South Australia, Mawson Lakes, SA 5082, Australia, and Department of Science and Technology, University of Linköping, S-601 74, Norrköping, Sweden

Received September 4, 2008. Revised Manuscript Received December 8, 2008

The cell-model electrokinetic theory of Ahualli et al. *Langmuir* **2006**, *22*, 7041; Ahualli et al. *J. Colloid Interface Sci.* **2007**, *309*, 342; and Bradshaw-Hajek et al. *Langmuir* **2008**, *24*, 4512 is applied to a dense suspension of charged spherical particles, to exhibit the system's dielectric response to an applied electric field as a function of solids volume fraction. The model's predictions of effective permittivity and complex conductivity are favorably compared with published theoretical calculations and experimental measurements on dense colloidal systems. Physical factors governing the volume fraction dependence of the dielectric response are discussed.

1. Introduction

In a recent series of papers,[1−3] the authors proposed a self-consistent cell-model theory of electrokinetics for concentrated suspensions of charged spherical particles. The cell-model theory, which is used to account approximately for electrical double layer interactions, is self-consistent in the sense that the model itself generates a natural set of boundary conditions through the application of physically motivated, volume-averaged constraints. To our knowledge, the cell-model provides the best means available of modeling electrical double layer interaction effects on the electrokinetics of concentrated charged particle systems. A more physically correct approach is the two-particle, perturbation method pursued by Ennis et al.[4,5] Unfortunately, in practice, this approach leads only to first-order, volume fraction dependent expressions for the dynamic mobility and dielectric properties, as only two-particle interactions are incorporated explicitly. There has not yet been an announcement in the literature, that we are aware of, of a more accurate approach to determining the effect of particle−particle interactions on the mobility, conductivity, and dielectric response of suspensions under general conditions. An alternate approach for low particle permittivity and high κa systems has been advanced by O'Brien et al.[6]

In our previous publications, attention focused on the influence of particle interactions on, first, the dynamic mobility of the particles[1,2] and, second, on the conductivity of the suspension.[3] The theoretical calculations of dynamic mobility were compared with experimental mobility measurements in ref 2, with quite reasonable agreement at both low (3%) and moderately high (25%) volume fractions of spherical silica particles in an aqueous electrolyte medium. It was thus demonstrated that the cell model is able to describe electrophoretic mobility measurements in concentrated systems.[2] Given that dielectric response measurements (conductivity and permittivity) appear to be a far more sensitive test, it is instructive to make a similar comparison with complex conductivity data. In this paper, we therefore supplement our electrokinetic cell-model analysis contained in refs 1−3 with information directed along three fronts. We compare our theoretical complex conductivity results with the published theoretical work of DeLacey and White[7] which is correct to order ϕ but limited to lower frequencies. We also apply our model calculations of the complex conductivity[3] to a number of dense colloidal systems that have been studied experimentally for which data on conductivity and permittivity is available in the literature.[8,9] Third, we examine the physical reasons for the dependence of the dielectric response on volume fraction.

Theories for the electrokinetics of dilute suspensions of spherical particles are well developed.[10−16] The standard model for calculating the complex conductivity of dilute suspensions in an oscillating field was developed by DeLacey and White,[7] based on the O'Brien and White[10] model for a static electric field. This theory has been tested experimentally by a number of authors (for example, see refs 17 and 18) for low volume fraction suspensions. In dilute suspensions, the particle contribution to the suspension's complex conductivity can be difficult to measure[19] because the particle contribution is approximately proportional to the concentration of particles. An electrokinetic theory valid for high volume fractions is therefore desirable.

† This work was supported by a grant from the Swedish Research Council.
‡ University of South Australia.
§ University of Linköping.

(1) Ahualli, S.; Delgado, A.; Miklavcic, S.; White, L. R. *Langmuir* **2006**, *22*, 7041.
(2) Ahualli, S.; Delgado, A.; Miklavcic, S.; White, L. R. *J. Colloid Interface Sci.* **2007**, *309*, 342.
(3) Bradshaw-Hajek, B. H.; Miklavcic, S. J.; White, L. R. *Langmuir* **2008**, *24*, 4512.
(4) Ennis, J.; Shugai, A. A.; Carnie, S. L. *J. Colloid Interface Sci.* **2000**, *223*, 21.
(5) Ennis, J.; Shugai, A. A.; Carnie, S. L. *J. Colloid Interface Sci.* **2000**, *223*, 37.
(6) O'Brien, R. W.; Jones, A.; Rowlands, W. N. *Colloids Surf., A* **2003**, *218*, 89.
(7) DeLacey, E. H. B.; White, L. R. *J. Chem. Soc. Faraday Trans. 2* **1981**, *77*, 2007.
(8) Midmore, B. R.; Hunter, R. J.; O'Brien, R. W. *J. Colloid Interface Sci.* **1987**, *120*, 210.
(9) Minor, M.; van Leeuwen, H. P.; Lyklema, J. *J. Colloid Interface Sci.* **1998**, *206*, 397.
(10) O'Brien, R. W.; White, L. R. *J. Chem. Soc. Faraday Trans. 2* **1978**, *74*, 1607.
(11) O'Brien, R. W. *J. Colloid Interface Sci.* **1986**, *113*, 81.
(12) O'Brien, R. W. *J. Fluid Mech.* **1988**, *190*, 71.
(13) O'Brien, R. W. *J. Fluid Mech.* **1990**, *212*, 81.
(14) Mangelsdorf, C. S.; White, L. R. *J. Chem. Soc. Faraday Trans.* **1992**, *88*, 3567.
(15) Rosen, L. A.; Baygents, J. C.; Saville, D. A. *J. Chem. Phys.* **1993**, *98*, 4183.
(16) Ennis, J.; White, L. R. *J. Colloid Interface Sci.* **1996**, *178*, 446.
(17) Rosen, L. A.; Saville, D. A. *J. Colloid Interface Sci.* **1990**, *140*, 82.
(18) Carrique, F.; Zurita, L.; Delgado, A. V. *J. Colloid Interface Sci.* **1994**, *166*, 128.
(19) Myers, D. F.; Saville, D. A. *J. Colloid Interface Sci.* **1989**, *131*, 448.

10.1021/la8028963 CCC: $40.75
Published on Web 01/20/2009

It is well-known that theoretical determinations of the frequency-dependent, complex permittivity do not always compare favorably with experiment, especially at the low frequency or static limit.[9,17,20] There are two plausible explanations for this discrepancy. The first is the failure to accurately correct impedance measurements for electrode polarization.[20,21] Second, since this discrepancy appears to be a general finding, independent of the particulars of the theoretical model employed, reasons that have been put forward refer to physical characteristics that have been excluded in the models, such as surface conduction or nonuniformity of the charge layer on the particle surface[18,20,22] rather than a failure of the models per se. One of the conclusions we draw from the comparison herein is that if it can be accepted that the self-consistent cell-model of electrokinetics is the best means available to account for particle interactions, then further investigation of the above-mentioned second order effects are indeed warranted, at least in some experimental situations.

A number of cell models have appeared in the literature (for example, see refs 23−25), differing only in the boundary conditions applied at the outer boundary. Historically, these boundary conditions have been invoked in an ad hoc manner. In our development of the cell model, we have taken the view that these boundary conditions must be derived from integral constraints over the suspension volume of the relevant physical quantities.[1−3] This philosophy is also shared by the authors of a recent treatment of the cell model approach to colloidal electrokinetics.[26]

2. Fundamental Equations

As described in detail in previous papers,[1−3] the electrokinetic response of a charged particle suspension to a macroscopic oscillating electric field, $E(t)$, is described by the following fundamental equations (see also refs 11−13):

$$\nabla^2\Psi(\mathbf{r},t) = -\frac{1}{\varepsilon_s\varepsilon_0}\rho_{ch}(\mathbf{r},t) \tag{1}$$

$$\rho_s\frac{\partial \mathbf{u}}{\partial t}(\mathbf{r},t) = -\nabla p(\mathbf{r},t) - \rho_{ch}(\mathbf{r},t)\nabla\Psi(\mathbf{r},t) + \eta_s\nabla^2\mathbf{u}(\mathbf{r},t) \tag{2}$$

$$\nabla\cdot\mathbf{u}(\mathbf{r},t) = 0 \tag{3}$$

$$\mathbf{v}_j(\mathbf{r},t) = \mathbf{u}(\mathbf{r},t) - \frac{1}{\lambda_j}\nabla\mu_j(\mathbf{r},t) \tag{4}$$

$$\frac{\partial n_j}{\partial t}(\mathbf{r},t) + \nabla\cdot[n_j(\mathbf{r},t)\mathbf{v}_j(\mathbf{r},t)] = 0 \tag{5}$$

$$\mu_j(\mathbf{r},t) = -z_je\Phi_j(\mathbf{r},t) = \mu_j^\infty + z_je\Psi(\mathbf{r},t) + k_BT\ln[n_j(\mathbf{r},t)] \tag{6}$$

with charge density

$$\rho_{ch}(\mathbf{r},t) = \sum_{j=1}^{N} z_jen_j(\mathbf{r},t) \tag{7}$$

Here, the electrolyte ion number densities are denoted n_j, the local charge density ρ_{ch}, the electrochemical potentials μ_j, the drift velocities $\mathbf{v}_j$, ($j = 1, 2,..., N$), the hydrodynamic flow field $\mathbf{u}$, the pressure p, and the electrostatic potential, Ψ. In addition, e, ε_s, ε_0, ρ_s, η_s, z_j, λ_j, k_B, and T are the electron charge, the fluid relative dielectric permittivity, vacuum permittivity, fluid mass density, fluid viscosity, valency and ionic drag coefficients of the jth ion type, Boltzmann constant, and temperature, respectively. The ion densities, n_j^∞, are those of the electrolyte reservoir in equilibrium with the field-free suspension. The drag coefficient, λ_j, is related to the ionic limiting conductance, Λ_j^∞, by

$$\lambda_j = \frac{N_Ae^2|z_j|}{\Lambda_j^\infty}$$

where N_A is Avogadro's number. The electrochemical potential functions $\Phi_j(\mathbf{r},t)$ describe the deviations of the local ion densities from their Poisson−Boltzmann expressions (see eq 6). For a more detailed explanation of these equations, see ref 1. The Debye parameter is given by

$$\kappa^2 = \sum_{j=1}^{N}\frac{e^2z_j^2n_j^\infty}{\varepsilon_s\varepsilon_0k_BT}$$

Under the influence of the volume averaged applied electric field, $\mathbf{E}$, oscillating at angular frequency ω, the field variables deviate from their equilibrium values.[11−13] The deviation is supposed sufficiently weak that only the first order perturbation correction in $\mathbf{E}$ is needed:

$$\Xi(\mathbf{r},t) = \Xi^{(0)}(\mathbf{r}) + \xi(r)\mathbf{E}\cdot\hat{\mathbf{r}}e^{-i\omega t} + O(\mathbf{E}(t)^2) \tag{8}$$

Here, Ξ represents any of the field variables, Φ_j, Ψ, ρ_{ch}, μ_j, n_j, and p, with $\Xi^{(0)}$ representing the respective field-independent equilibrium contributions. The first order correction, $\xi(r)$, represents any of the functions, $\psi(r)$, $\phi_j(r)$, and $P(r)$, which correspond to perturbations to the electrostatic potential, electrochemical potential, and the hydrodynamic pressure, respectively. Symmetry ensures that the perturbed fluid velocity will have the form (in the reference frame of the central particle)[27]

$$\mathbf{u}(\mathbf{r}) = (u_r, u_\theta, u_\phi) = \mu(\omega)\mathbf{E} - \left(\frac{2h(r)}{r}\mathbf{E}\cdot\hat{\mathbf{r}}, \frac{1}{r}\frac{\partial(rh(r))}{\partial r}[\mathbf{E} - \mathbf{E}\cdot\hat{\mathbf{r}}\hat{\mathbf{r}}]\cdot\hat{\theta}, 0\right) \tag{9}$$

where $\mu(\omega)$ is the dynamic mobility and $h(r)$ is a flow field function.

Invoking the perturbation expansion eq 8 in the fundamental system (eqs 1−7) leads to a zeroth-order and a first-order system of equations. The zeroth-order contributions satisfy the field equations

$$\begin{cases} n_j^{(0)}(r) = n_j^\infty\exp(-z_je\Psi^{(0)}(r)/k_BT) \\ \rho_{ch}^{(0)}(r) = \sum_{j=1}^{N} z_jen_j^{(0)}(r) \end{cases}$$
$$p^{(0)}(r) = p_{amb} + \sum_{j=1}^{N}(n_j^{(0)}(r) - n_j^\infty)k_BT \tag{10}$$
$$\mu_j^{(0)}(r) = -z_je\Phi_j^{(0)}(r) = \mu_j^\infty + k_BT\ln n_j^\infty$$

and

(20) Jiménez, M. L.; Arroyo, F. J.; van Turnhout, J.; Delgado, A. V. *J. Colloid Interface Sci.* **2002**, *249*, 327.
(21) Hollingsworth, A. D.; Saville, D. A. *J. Colloid Interface Sci.* **2003**, *257*, 65.
(22) Hill, R. J.; Saville, D. A.; Russel, W. B. *J. Colloid Interface Sci.* **2003**, *263*, 478.
(23) Kozak, M. W.; Davis, E. J. *J. Colloid Interface Sci.* **1986**, *112*, 403.
(24) Shilov, V. N.; Zharkikh, N. I.; Borkovskaya, Y. B. *Kolloidn. Zh.* **1981**, *43*, 434.
(25) Dukhin, A. S.; Shilov, V. N.; Ohshima, H.; Goetz, P. J. *Langmuir* **1999**, *15*, 6692.
(26) Zholkovskij, E. K.; Masliyah, J. H.; Shilov, V. N.; Bhattacharjee, S. *Adv. Colloid Interface Sci.* **2007**, *134*, 279.
(27) Landau, L. D. Lifshitz, E. M. *Fluid Mechanics*; Pergamon Press: Oxford, 1966.

$$\frac{1}{r^2}\frac{\mathrm{d}}{\mathrm{d}r}\left(r^2\frac{\mathrm{d}\Psi^{(0)}}{\mathrm{d}r}(r)\right)=\begin{cases}0, & r<a\\ -\dfrac{\rho_{\mathrm{ch}}^{(0)}(r)}{\varepsilon_{\mathrm{s}}\varepsilon_0}, & a<r<b\end{cases}$$

subject to the following conditions. At the slipping plane at each particle surface, $r = a$,

$$\Psi^{(0)}|_{r=a}=\zeta$$

while global electroneutrality leads to the condition[2]

$$\left.\frac{\mathrm{d}\Psi^{(0)}}{\mathrm{d}r}\right|_{r=b}=0$$

at the cell wall. In eq 10, p_{amb} is the ambient pressure in the reservoir that is in equilibrium with the suspension.

The first-order problem involves the following coupled set of complex ordinary differential equations for the functions ψ, ϕ_j, and h[14]

$$L\psi(r)=\frac{e^2}{\varepsilon_{\mathrm{s}}\varepsilon_0 k_{\mathrm{B}}T}\sum_{j=1}^{N}z_j^2n_j^{(0)}(r)[\phi_j(r)+\psi(r)]$$

$$L\phi_j(r)+\gamma_j^2[\phi_j(r)+\psi(r)]=\frac{e}{k_{\mathrm{B}}T}\frac{\mathrm{d}\Psi^{(0)}}{\mathrm{d}r}(r)\left(z_j\frac{\mathrm{d}\phi_j(r)}{\mathrm{d}r}-\frac{2\lambda_j}{e}\frac{h(r)}{r}\right)$$

and

$$L(L+\gamma^2)h(r)=-\frac{e^2}{\eta_s k_{\mathrm{B}}T}\frac{1}{r}\frac{\mathrm{d}\Psi^{(0)}}{\mathrm{d}r}\sum_{j=1}^{N}z_j^2n_j^{(0)}(r)\phi_j(r)$$

with complex constants

$$\gamma=\frac{(1+i)}{\sqrt{2}}\sqrt{\frac{\omega\rho_{\mathrm{s}}}{\eta_s}},\quad \gamma_j=\frac{(1+i)}{\sqrt{2}}\sqrt{\frac{\omega\lambda_j}{k_{\mathrm{B}}T}}$$

and the second-order differential operator

$$L=\frac{\mathrm{d}^2}{\mathrm{d}r^2}+\frac{2}{r}\frac{\mathrm{d}}{\mathrm{d}r}-\frac{2}{r^2}$$

This system must satisfy the following boundary conditions.[14] At $r = a$,

$$h(a)=\left.\frac{\mathrm{d}h}{\mathrm{d}r}\right|_{r=a}=0$$

$$\left.\frac{\mathrm{d}\phi_j}{\mathrm{d}r}\right|_{r=a}=0$$

and

$$\left.\frac{\mathrm{d}\psi}{\mathrm{d}r}\right|_{r=a}-\frac{\varepsilon_{\mathrm{p}}}{\varepsilon_{\mathrm{s}}a}\psi(a)=0$$

At r = b,

$$\psi(b)=-b$$

$$\phi_j(b)=b$$

$$Lh|_{r=b}=0$$

and

$$\left.\frac{\mathrm{d}}{\mathrm{d}r}[(L+\gamma^2)h]\right|_{r=b}=\frac{\gamma^2h(b)}{b}\frac{\left(1-\phi\dfrac{\Delta\rho}{\rho_{\mathrm{s}}}\right)}{\left(1+\phi\dfrac{\Delta\rho}{\rho_{\mathrm{s}}}\right)}+\frac{\rho_{\mathrm{ch}}^{(0)}(b)}{\eta_{\mathrm{s}}}$$

The dynamic mobility, used in deriving the above, is found to be

$$\mu=\frac{2h(b)}{b}\left[1+\phi\frac{\Delta\rho}{\rho_{\mathrm{s}}}\right]^{-1}$$

More explicit details of the above derivation and details of our numerical calculation can be found in refs 1−3. A user-friendly program for calculating the conductivity and dielectric response of a suspension is available from the authors.

3. Admittance and Complex Conductivity

Permittivity data are usually obtained through measurements of complex admittance based on electric field response experiments. As described by DeLacey and White,[7] for a parallel plate arrangement, the admittance is related directly to the complex conductivity through the formula

$$Y(\omega)=\frac{A}{d}K^*(\omega)$$

where A is the plate area and d is the plate spacing. By means of this equation, a model of complex conductivity can be directly compared with experiment.

In an earlier paper,[3] we derived an expression for the complex conductivity, K^*, of a concentrated charged particle suspension based on the definition $\langle\mathbf{i}\rangle = K^*\mathbf{E}$. In terms of the perturbed variables introduced above and based on our self-consistent cell model, we deduced the complex conductivity to be

$$K^*=-\rho_{\mathrm{ch}}^{(0)}(b)\mu\phi\frac{\Delta\rho}{\rho_{\mathrm{s}}}+\sum_{j=1}^{N}\frac{z_j^2e^2n_j^{(0)}(b)}{\lambda_j}\frac{\mathrm{d}\phi_j}{\mathrm{d}r}(b)\times\exp\left(\frac{-z_je\Psi^{(0)}(b)}{k_{\mathrm{B}}T}\right)+i\omega\varepsilon_{\mathrm{s}}\varepsilon_0\frac{\mathrm{d}\psi}{\mathrm{d}r}(b)$$

which, in addition to a contribution from the dispersed particles and their associated electrical double layers, contains a contribution from the bulk electrolyte,

$$K_{\mathrm{sol}}^*=\sum_{j=1}^{N}\frac{z_j^2e^2n_j^{\infty}}{\lambda_j}-i\omega\varepsilon_{\mathrm{s}}\varepsilon_0$$

Consequently, attention was focused on the difference between these two quantities, $\Delta K^*(\omega, \phi) = K^* - K_{\mathrm{sol}}^*$, representing the departure from the bulk conductivity

$$\Delta K^*(\omega,\phi)=\sum_{j=1}^{N}\frac{z_j^2e^2n_j^{\infty}}{\lambda_j}\left[\exp\left(\frac{-z_je\Psi^{(0)}(b)}{k_{\mathrm{B}}T}\right)\frac{\mathrm{d}\phi_j}{\mathrm{d}r}(b)-1\right]-\rho_{\mathrm{ch}}^{(0)}(b)\mu\phi\frac{\Delta\rho}{\rho_{\mathrm{s}}}+i\omega\varepsilon_{\mathrm{s}}\varepsilon_0\left[\frac{\mathrm{d}\psi}{\mathrm{d}r}(b)+1\right] \quad (11)$$

From the imaginary part of this complex conductivity increment, it is customary to obtain the real part of the dielectric permittivity increment as

$$\Delta\varepsilon'(\omega,\phi)=\frac{-\mathrm{Im}(\Delta K^*(\omega,\phi))}{\omega\varepsilon_0} \quad (12)$$

At this stage of the theoretical development many authors (for example refs 7 and 28−30)—in fact most authors—consider a perturbation expansion of $\Delta K^*(\omega, \phi)$ and extract from eq 11 a first-order, volume fraction dependence,

$$\Delta K^*(\omega,\phi)=\Delta K^*(\omega)\phi+O(\phi^2)$$

(Note, however, that in our current and previous work,[3] no linear factor of ϕ has been extracted from the expression for the complex

(28) Carrique, F.; Criado, C.; Delgado, A. V. *J. Colloid Interface Sci.* **1993**, *156*, 117.

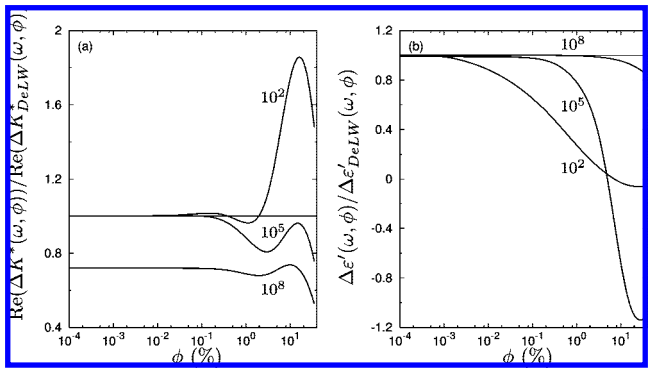

Figure 1. (a) $Re(\Delta K^*(\omega, \phi))/Re(\Delta K^*_{DeLW}(\omega, \phi))$ and (b) $\Delta\varepsilon'(\omega, \phi)/\Delta\varepsilon_{DeLW}'(\omega, \phi)$ as functions of volume fraction at frequencies $\omega/2\pi = 10^2$, 10^5, and 10^8 Hz for $\kappa a = 1$ and $\zeta = 100$ mV.

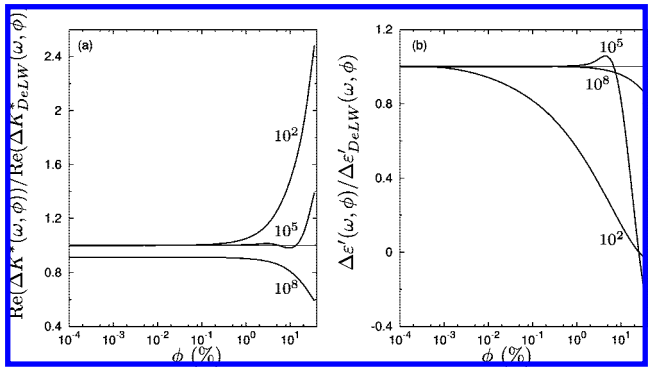

Figure 2. (a) $Re(\Delta K^*(\omega, \phi))/Re(\Delta K^*_{DeLW}(\omega, \phi))$ and (b) $\Delta\varepsilon'(\omega, \phi)/\Delta\varepsilon_{DeLW}'(\omega, \phi)$ as functions of volume fraction at frequencies $\omega/2\pi = 10^2$, 10^5, and 10^8 Hz for $\kappa a = 5$ and $\zeta = 100$ mV.

conductivity increment. This allows us to explicitly include second and higher-order volume fraction dependencies.) These authors then express the coefficient of the first order volume fraction term as the sum of a (real) conductivity increment $\Delta K(\omega)$ and a (complex) dielectric response increment, $\Delta\varepsilon(\omega) = \Delta\varepsilon'(\omega) + i\Delta\varepsilon''(\omega)$:

$$\Delta K^*(\omega) = [\Delta K(\omega) + \omega\varepsilon_0\Delta\varepsilon''(\omega)] - i\omega\varepsilon_0\Delta\varepsilon'(\omega) \quad (13)$$

where $\Delta\varepsilon'(\omega)$ is the frequency dependent measure of the strength of polarization of the dispersion and $i\Delta\varepsilon''(\omega)$ is the dielectric loss. As recognized by many authors,[7,28,30,31] it is typically these latter quantities, $\Delta\varepsilon'(\omega)$ and $\Delta\varepsilon''(\omega)$, that are compared with experiment. DeLacey and White[7] note that there is no way to separate the two contributions to the experimentally measured quantity $[\Delta K(\omega) + \omega\varepsilon_0\Delta\varepsilon''(\omega)]$. In fact, two different interpretations of this quantity exist, both used by experimentalists.[7] One interpretation is to deny the existence of the dielectric loss term, and attribute all frequency dependence to the conductance increment. However, more commonly, experimentalists attribute all frequency dependence to the dielectric loss term, inferring that the conductivity contribution is actually the static value, i.e. $\Delta K(\omega) = \Delta K(0)$. This view is supported by the work of Carrique, et al.[28] in which the quantity $\Delta\varepsilon''(\omega)$ is calculated via the Kramers−Krönig relations from the $\Delta\varepsilon'(\omega)$ expression.

4. Results and Discussion

In this section, results of calculations based on the present model are presented in three different contexts. First, our dielectric permittivity and conductivity calculations are compared with the theoretical results of DeLacey and White,[7] which is the model calculation most commonly referred to in the literature. Second, our model calculations are compared with the experimentally measured dielectric permittivities and conductivities published by Midmore et al.[8] and Minor et al.[9] For our examination of this experimental data, we use the dielectric permittivity increment as calculated using eq 12. Finally, the physical factors governing the volume fraction dependence of the dielectric response are discussed.

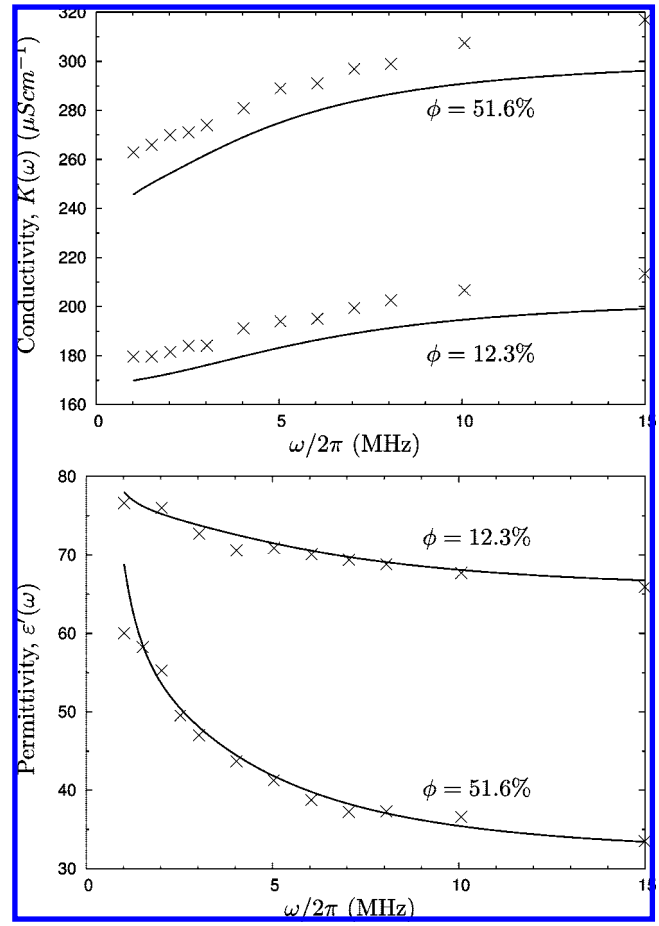

Figure 3. (a) Conductivity and (b) permittivity of a polystyrene latex suspension at two different volume fractions. Crosses represent the experimental results (from ref 8), and the solid lines show theoretical results using the present theory with $\zeta = -162$ mV for spherical particles, $a = 253$ nm, in a KCl solution (10^{-3} M) at $T = 25$ °C.

In the choice of systems with which we compare the cell-model theory, we have attempted to cover a wide parameter range of ζ-potential, κa, and volume fraction values. The comparison thus provides some indication of the relative accuracy of the model under a wide range of conditions.

4.1. Comparison with DeLacey and White. DeLacey and White[7] developed and solved a low volume fraction, low frequency approximation model of electrokinetics based on the same standard electrokinetic equations that govern the behavior of suspensions in an oscillating electric field (see section 2). The conductivity and dielectric permittivity increments were then determined to first order in volume fraction. However, as Carrique, et al.[32,33] note, it is difficult to establish experimentally a linearly

(29) Barchini, R.; Saville, D. A. *J. Colloid Interface Sci.* **1995**, *173*, 86.
(30) Hill, R. J.; Saville, D. A.; Russel, W. B. *J. Colloid Interface Sci.* **2003**, *268*, 230.
(31) Mangelsdorf, C. S.; White, L. R. *J. Chem. Soc. Faraday Trans.* **1997**, *93*, 3145.
(32) Carrique, F.; Arroyo, F. J.; Jiménez, M. L.; Delgado, A. V. *J. Chem. Phys.* **2003**, *118*, 1945.

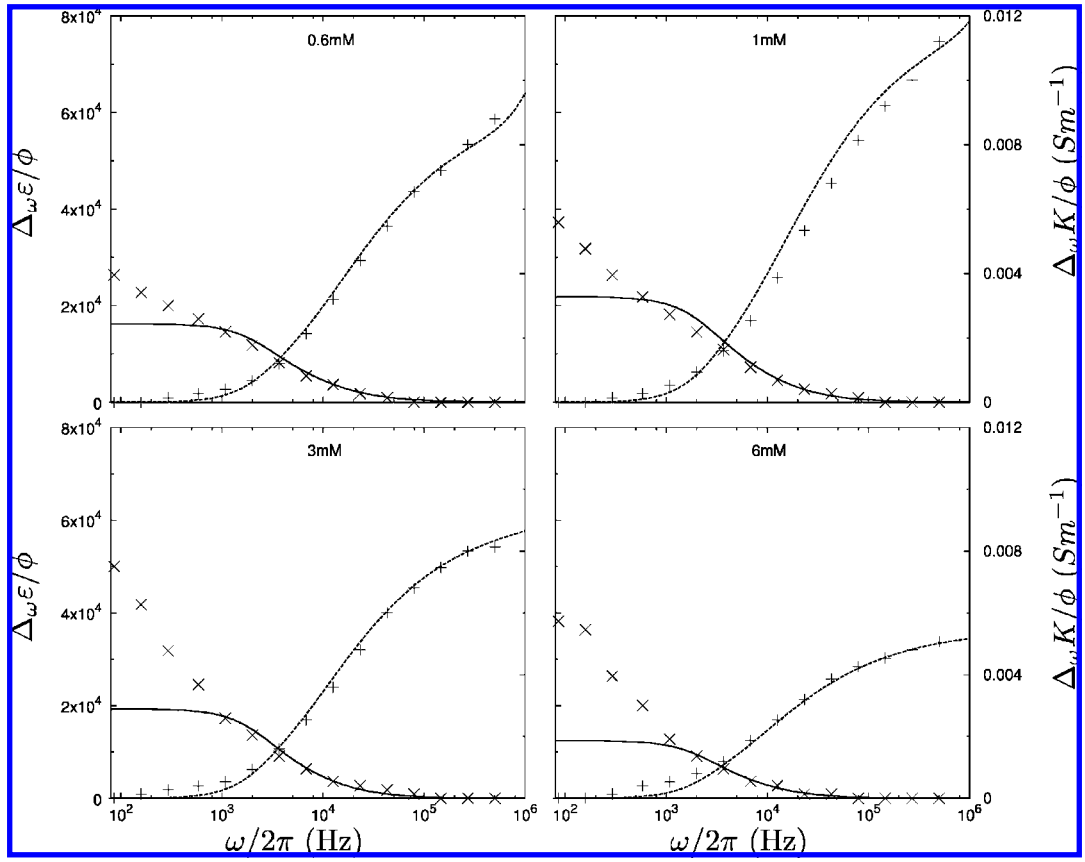

Figure 4. Conductivity and permittivity increments for a polystyrene sulfate latex suspension at four different electrolyte concentrations. Symbols represent the experimental results of Minor et al.[9] (permittivity increments ×, conductivity increments +), and lines represent results from the current theory (solid lines are permittivity increments, dashed lines are conductivity increments). Spherical particles, $a = 400$ nm in KCl solution at $T = 25$ °C, $\phi = 2\%$.

dependent region. Nevertheless, as the DeLacey and White[7] paper is often referred to in this field, it is appropriate to establish our results against this benchmark.

Other favorable comparisons with the DeLacey and White[7] model include: the mobility calculations of Mangelsdorf and White[14] (their inclusion of inertia demonstrated that the DeLacey and White model was accurate for frequencies less than 10^5 Hz); the dipole coefficient calculations of Mangelsdorf and White;[31] the analytical permittivity and dipole coefficient calculations of Shilov et al.;[34] the comparison of Fixman's[35] approximate theory for the dielectric response valid for $\kappa a \gg 1$ by Carrique et al.;[36] and the experimental conductivity and permittivity measurements of Hollingsworth and Saville.[37]

The two approximations inherent in the DeLacey and White model are the neglect of the inertial term $\rho_s\ \partial\mathbf{u}/\partial t$ in the hydrodynamics and the restriction to $O(\phi)$ terms in the volume fraction dependence. It is important to appreciate that the frequency dependence of the ion motions is treated correctly in that model. Our cell model does not possess these limitations. In Figure 1, we plot (a) $\mathrm{Re}(\Delta K^*(\omega, \phi))/\mathrm{Re}(\Delta K^*_{\mathrm{DeLW}}(\omega, \phi))$ and (b) $\Delta\varepsilon'(\omega, \phi)/\Delta\varepsilon_{\mathrm{DeLW}}'(\omega, \phi)$ as functions of volume fraction at three frequencies $\omega/2\pi = 10^2$, 10^5, and 10^8 Hz for $\kappa a = 1$ and $\zeta = 100$ mV. We note that the real part is well approximated by the DeLacey and White model for volume fractions $\phi < 0.1\%$ for the frequencies 10^2 and 10^5 Hz where the inertial approximation is unimportant, but at the high frequency of 10^8 Hz, the neglect of inertia is important at all volume fractions. The permittivity comparison (Figure 1b) shows agreement between the theories up to 0.1% for the higher frequencies and 0.001% for the low frequency. The deviation in Figure 1b at the low frequency demonstrates the importance of the dynamic ion distribution on the cell polarizability. When ion diffusion lengths are longer than the cell dimension, as in the low frequency case, the overlap of the perturbed ion densities is not accounted for in the DeLacey and White treatment. In Figure 2, we plot the same comparisons but for a thinner equilibrium double layer $\kappa a = 5$. These plots show similar behavior to the $\kappa a = 1$ case, but the region of agreement between the theories shifts to ~1% which is to be expected since particle−particle interaction is reduced in the thinner double layer situation.

4.2. Comparison with Experimental Data. In the work of Midmore et al.,[8] the authors developed an approximate formula for the complex conductivity of a suspension under thin double layer conditions, based on a related cell model. They compared this with experimentally measured values for the conductivity and permittivity of high volume fraction polystyrene latex suspensions. The latter physical system provides a close-to-ideal situation with which to compare the present model's predictions. In the following comparison with experimental data, it is important to recognize that we are free to treat only the ζ-potential as an adjustable parameter. Figure 3 shows that good agreement between theory (lines) and experiment (data points) can be obtained—simultaneously for both quantities, conductivity and

(33) Arroyo, F. J.; Carrique, F.; Jiménez, M. L.; Delgado, A. V. *Ann. Univ. Mariae Curie-Sklodowska Sect. AA Chem.* **2005**, *60*, 1.
(34) Shilov, V. N.; Delgado, A. V.; Gonzalez-Caballero, F.; Grosse, C. *Colloids Surf., A* **2001**, *192*, 253.
(35) Fixman, M. *J. Chem. Phys.* **1983**, *78*, 1483.
(36) Carrique, F.; Zurita, L.; Delgado, A. V. *J. Colloid Interface Sci.* **1995**, *170*, 176.
(37) Hollingsworth, A. D.; Saville, D. A. *J. Colloid Interface Sci.* **2004**, *272*, 235.

permittivity, and at both volume fractions (12.3% and 51.6%)—assuming a ζ-potential value of −159.3 mV as found by Midmore et al.

In the work of Minor et al.,[9] the authors presented experimentally measured values of the conductivity and permittivity increments for suspensions of polystyrene sulfate latex particles. Minor et al. defined the conductivity and permittivity increments as

$$\Delta_\omega K(\omega,\phi) = K(\omega,\phi) - K(0,\phi)$$
$$\Delta_\omega \varepsilon(\omega,\phi) = \varepsilon'(\omega,\phi) - \varepsilon'(\infty,\phi)$$

that is, the conductivity is measured relative to the static value and the permittivity is measured relative to the high frequency limiting value. Again, following the work of Minor et al.,[9] we present these increments normalized by ϕ. Figure 4 shows the experimental results of Minor et al. (symbols) and the corre-

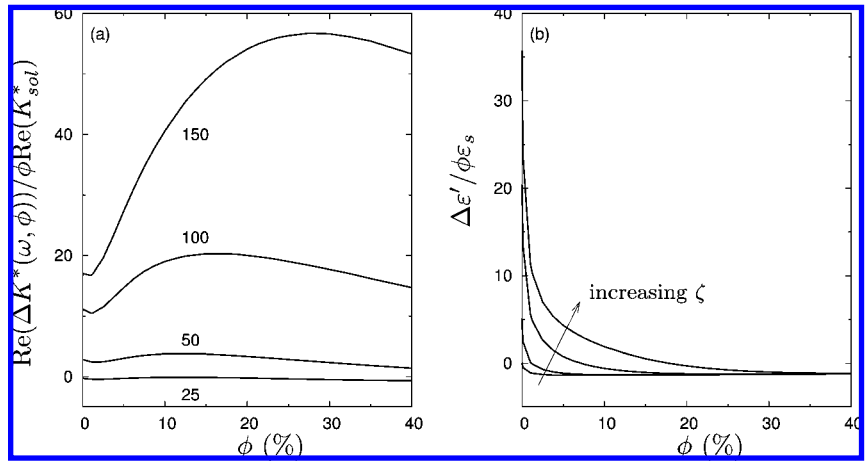

Figure 5. (a) $\mathrm{Re}(\Delta K^*(\omega,\phi))/\phi\mathrm{Re}(K^*_{sol})$ and (b) $\Delta\varepsilon'/\phi\varepsilon_s$ as functions of volume fraction ϕ for $\kappa a = 1$ and $\zeta = 25$, 50, 100, and 150 mV, for frequency $\omega/2\pi = 10^2$ Hz.

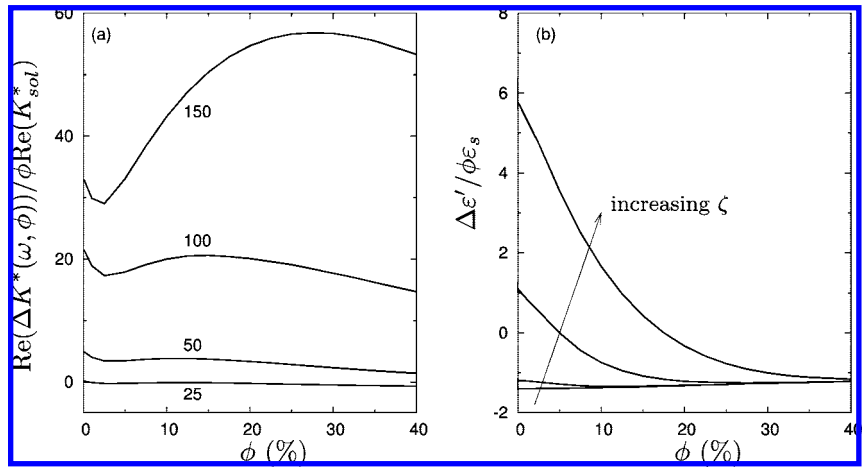

Figure 6. (a) $\mathrm{Re}(\Delta K^*(\omega,\phi))/\phi\mathrm{Re}(K^*_{sol})$ and (b) $\Delta\varepsilon'/\phi\varepsilon_s$ as functions of volume fraction ϕ for $\kappa a = 1$ and $\zeta = 25$, 50, 100, and 150 mV, for frequency $\omega/2\pi = 10^5$ Hz.

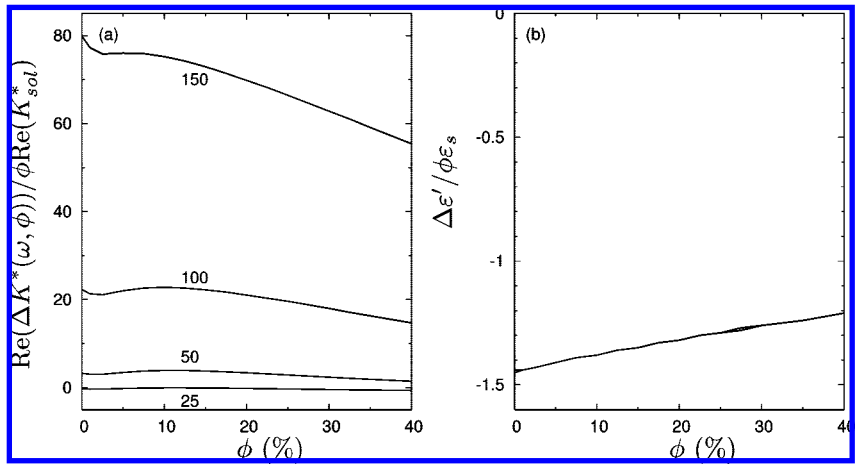

Figure 7. (a) $\mathrm{Re}(\Delta K^*(\omega,\phi))/\phi\mathrm{Re}(K^*_{sol})$ and (b) $\Delta\varepsilon'/\phi\varepsilon_s$ as functions of volume fraction ϕ for $\kappa a = 1$ and $\zeta = 25$, 50, 100, and 150 mV, for frequency $\omega/2\pi = 10^8$ Hz. In part b, the curves for different ζ are indistinguishable.

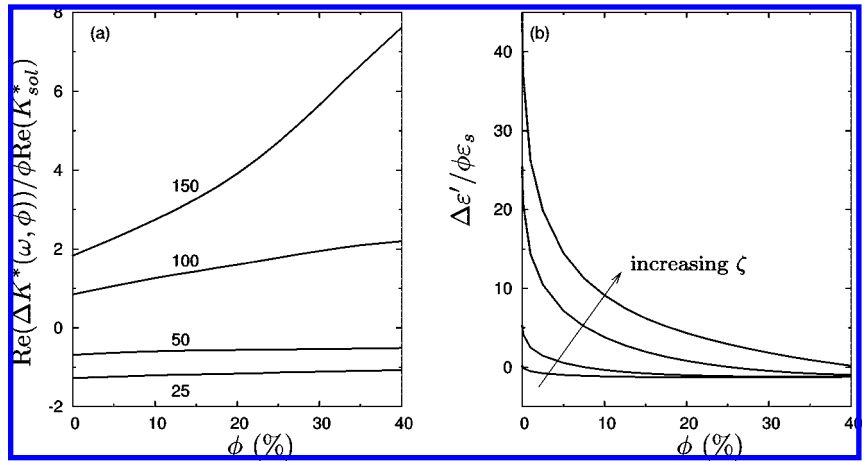

Figure 8. (a) $\mathrm{Re}(\Delta K^*(\omega, \phi))/\phi\mathrm{Re}(K^*_{\mathrm{sol}})$ and (b) $\Delta\varepsilon'/\phi\varepsilon_{\mathrm{s}}$ as functions of volume fraction ϕ for $\kappa a = 5$ and $\zeta = 25$, 50, 100, and 150 mV, for frequency $\omega/2\pi = 10^2$ Hz.

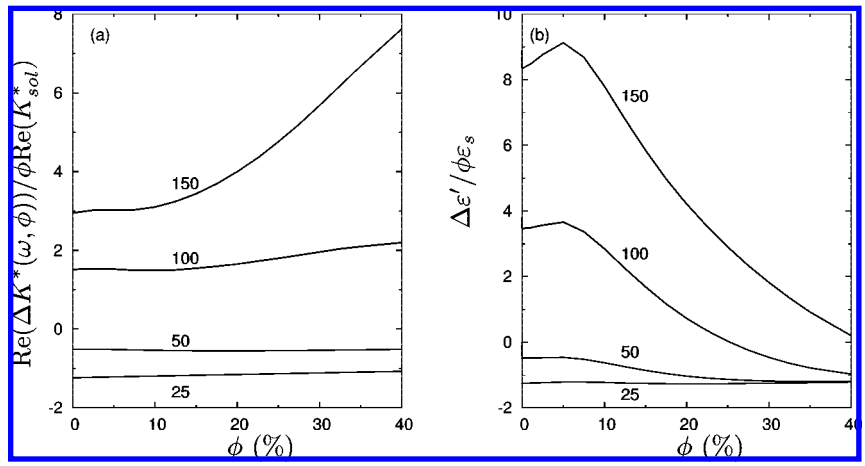

Figure 9. (a) $\mathrm{Re}(\Delta K^*(\omega, \phi))/\phi\mathrm{Re}(K^*_{\mathrm{sol}})$ and (b) $\Delta\varepsilon'/\phi\varepsilon_{\mathrm{s}}$ as functions of volume fraction ϕ for $\kappa a = 5$ and $\zeta = 25$, 50, 100, and 150 mV, for frequency $\omega/2\pi = 10^5$ Hz.

sponding predictions of the current model (lines). Once again, the ζ-potential value was treated as the only adjustable parameter. The ζ-potentials used to calculate the theoretical results presented here were $\zeta = -175$ mV ($c = 0.6$ mM and $c = 1$ mM), $\zeta = -145$ mV ($c = 3$ mM), and $\zeta = -125$ mV ($c = 6$ mM). It is unclear how these values compare with those effectively adopted by Minor et al.[9] as their model used a surface conductivity parameter rather than the ζ-potential of the particles. On the other hand, the values adopted here are not unrealistic, nor are the trends with added electrolyte. The results do suggest, though, that the ζ-potential is dependent on the electrolyte concentration.

For the conductivity, there is good agreement between theory and experiment over a large frequency range. There is similar and simultaneous good agreement between permittivity values, except at very low frequencies where the model predicts lower permittivities than those measured. This low frequency discrepancy is most likely caused by the experimental difficulty of accurately removing the electrode polarization effects in this frequency range.

However, similar discrepancies between experimentally measured and theoretically calculated permittivities are well-documented[9,17,18,20] and ascribed to the neglect of a dynamic Stern layer. There does appear to be a correlation between these discrepancies and the presence of complex particle surface properties (such as surface roughness or hairiness).

4.3. Volume Fraction Dependence of the Dielectric Response. The cell model may be expected to work best when there is significant double layer interaction between particles over a reasonable fraction of the particle surface. When the electrostatic interaction is confined to small, local regions on the particle, the smearing of the effect of neighboring particles is most likely to be in error. Of course at high κa values, the absence of overlap in equilibrium and perturbation fields, except at the highest volume fractions, means that the cell model treatment should not lead to serious error anyway. High κa theories that avoid the cell model and exploit this nonoverlap already exist.[6] The utility of the cell model is most likely to be found in the low κa regime where other approaches are not easily applied.

The physical factors governing the frequency dependence of the dielectric response of a colloidal suspension have been discussed by many authors[11−14,28,33,38] and will not be repeated here except where the additional length scale b of the cell model interacts with the length scales a, κ^{-1}, γ^{-1}, γ_j^{-1} of the isolated colloidal particle problem. In Figures 5−7, we plot (a) $\Delta K/(\phi K_{\mathrm{sol}})$ and (b) $\Delta\varepsilon'/(\phi\varepsilon_{\mathrm{s}})$ as functions of volume fraction ϕ (for $\kappa a = 1$ and a range of zeta potentials $\zeta = 25$, 50, 100, and 150 mV) for three frequencies $\omega/2\pi = 10^2$, 10^5, and 10^8 Hz. The κa value was chosen to accentuate the effect of equilibrium double layer overlap, and the zeta potential range was chosen to span the experimentally observed range. Note that in low

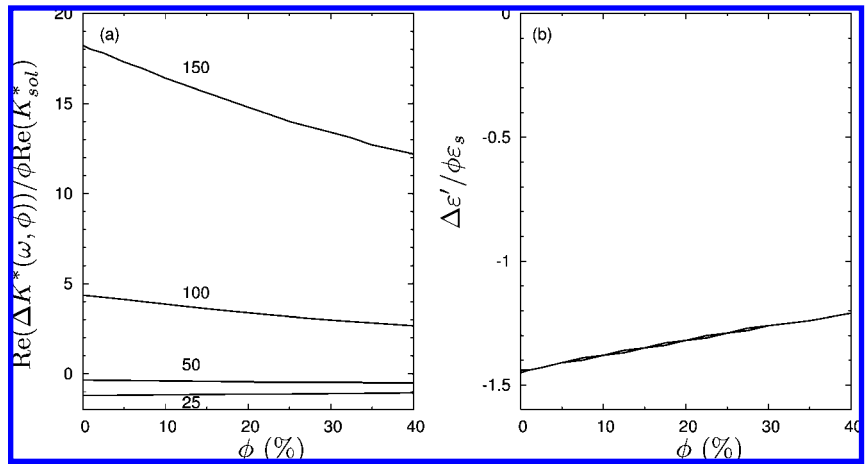

Figure 10. (a) $\mathrm{Re}(\Delta K^*(\omega,\phi))/\phi\mathrm{Re}(K^*_{sol})$ and (b) $\Delta\varepsilon'/\phi\varepsilon_s$ as functions of volume fraction ϕ for $\kappa a = 5$ and $\zeta = 25$, 50, 100, and 150 mV, for frequency $\omega/2\pi = 10^8$ Hz. In part b, the curves for different ζ are indistinguishable.

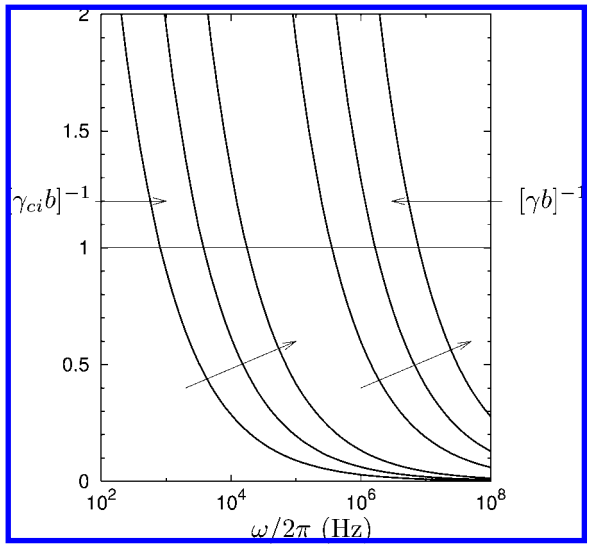

Figure 11. Hydrodynamic penetration depth and counterion diffusion length relative to cell dimension b, $[\gamma b]^{-1}$, and $[\gamma_{ci}b]^{-1}$, for $\phi = 0.4\%$, 4%, and 40%. Arrows show the direction of increasing volume fraction.

κa systems higher zeta values are common. In Figures 8−10, we plot the equivalent calculations for a thinner double layer system $\kappa a = 5$.

The frequencies were chosen to span the experimental range from essentially static situations through the accousticiser range and beyond and cover a considerable variation of the relevant length scales. In Figure 11, we show the hydrodynamic penetration depth and the counterion diffusion length relative to the particle−particle spacing $[\gamma b]^{-1}$, $[\gamma_{ci}b]^{-1}$ as a function of frequency for volume fractions $\phi = 0.4$, 4, and 40%. We observe that the ion diffusion length moves inside the cell boundary at $\sim 10^4$ Hz, the changeover frequency increasing with volume fraction whereas the hydrodynamic penetration depth moves inside the cell boundary at $\sim 3 \times 10^6$ Hz. Thus, at the low frequency of 10^2 Hz, both the ion diffusion length and hydrodynamic penetration depth are larger than the cell dimension while at 10^8 Hz, both length scales are far inside the cell boundary. For the intermediate frequency of 10^5 Hz, the ion diffusion length is well within and the hydrodynamic penetration depth outside the cell boundary. Figures 5−7 for $\kappa a = 1$ and Figures 8−10 for $\kappa a = 5$ show the result of this changeover of dominant length scale.

We can understand the ϕ dependence of $\mathrm{Re}(\Delta K^*)$ at low frequency (Figure 5a) if we estimate the conductance of the excess double layer ions in the equilibrium cell model. The equilibrium excess of ionic species j in the cell is

$$\Gamma j(\phi) = 4\pi n_j^\infty \int_a^b \mathrm{d}r\, r^2[\exp(-z_j e\Psi^{(0)}(r)/k_\mathrm{B}T) - 1]$$

and an estimate of the conductance of these ions is given by

$$\Delta K_{\mathrm{edl}}(\phi) = \left(\frac{\phi}{V_\mathrm{p}}\right)\sum_{j=1}^{N}\Gamma_j(\phi)\Lambda_j^\infty$$

where V_p is the volume of a particle. We define the dilute limit of this quantity as

$$\Delta K_{\mathrm{edl}}(0) = \left(\frac{\phi}{V_\mathrm{p}}\right)\sum_{j=1}^{N}\Gamma_j(0)\Lambda_j^\infty$$

where $\Gamma_j(0)$ is the excess around an isolated particle under the same zeta potential and reservoir electrolyte conditions. The difference between $\Delta K_{\mathrm{edl}}(\phi)$ and $\Delta K_{\mathrm{edl}}(0)$ is a measure of the effect of equilibrium double layer overlap on excess conductivity. Due to equilibrium double layer overlap as the volume fraction increases, the ion excesses change and hence so does ΔK_{edl}. In Figure 12, we plot $\Delta K_{\mathrm{edl}}(\phi)/\Delta K_{\mathrm{edl}}(0)$ and the relative equilibrium surface charge density $\sigma^{(0)}(\phi)/\sigma^{(0)}(0)$ for (a) various κa values ($\zeta = 100$ mV) and (b) for various ζ values ($\kappa a = 1$). We see that for $\kappa a = 1$, the normalized excess double layer conductance $\Delta K_{\mathrm{edl}}(\phi)/\Delta K_{\mathrm{edl}}(0)$ exhibits a maximum for all zeta potentials and this maximum is reflected in the normalized cell model conductivity increment $\Delta K(\omega,\phi)/(\phi K_{\mathrm{sol}})$ (see Figure 5a). If the dilute theory of DeLacey and White was valid at all ϕ, the plots in Figure 5a would be horizontal. As expected, the magnitude of the equilibrium surface charge density decreases monotonically as the double layer overlap increases. This result is analogous to the constant potential approach of two interacting double layers where the surface charge magnitude is driven lower on decrease of intersurface separation. At $\kappa a = 5$, $\Delta K_{\mathrm{edl}}(\phi)/\Delta K_{\mathrm{edl}}(0)$ is significantly smaller than the $\kappa a = 1$ case and increases monotonically over the volume fraction range plotted. Again this behavior is reflected in the cell model conductivity increment $\mathrm{Re}(\Delta K^*(\omega,\phi))/\phi\mathrm{Re}(K^*_{\mathrm{sol}})$. Note that the ratio $\Delta K_{\mathrm{edl}}/\Delta K_{\mathrm{edl}}(0)$ decreases with increasing zeta potential (since $\Gamma_j(0)$ is a stronger function of ζ than $\Gamma_j(\phi)$) but the value of $\Delta K_{\mathrm{edl}}(\phi)$ increases with

(38) Dukhin S.S., Shilov V. N., *Dielectric phenomena and the double layer in disperse systems and polyelectrolytes*; Wiley: New York, 1974.

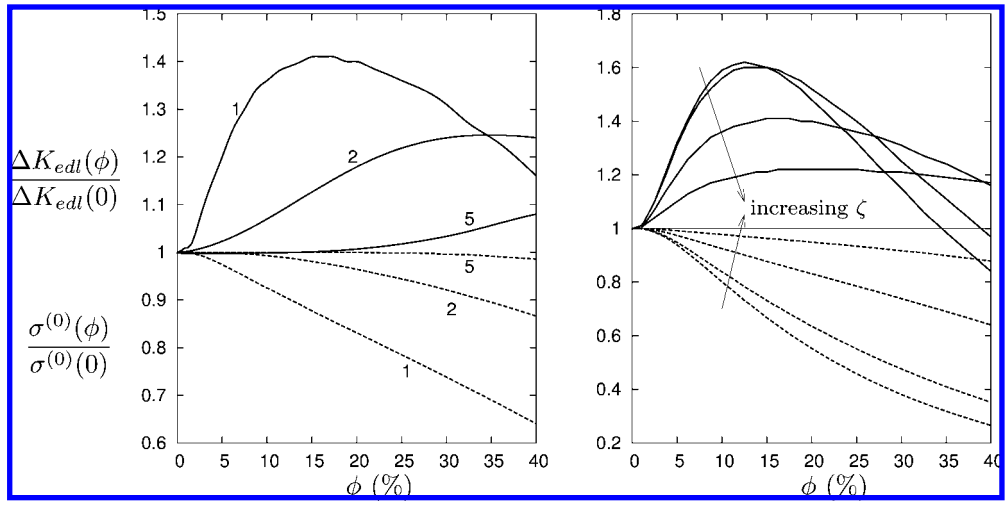

Figure 12. $\Delta K_{edl}(\phi)/\Delta K_{edl}(0)$ (solid lines) and the relative equilibrium surface charge density $\sigma^{(0)}(\phi)/\sigma^{(0)}(0)$ (dotted lines) for (a) various κa values ($\zeta = 100$ mV) and (b) for various ζ values, $\zeta = 20$, 50, 100, and 150 mV ($\kappa a = 1$).

zeta potential. Accordingly, $\mathrm{Re}(\Delta K^*(\omega,\phi))/\phi\mathrm{Re}(K^*_{sol})$ (see Figures 5a and 8a) increases with ζ as expected.

In Figure 5b, the low frequency permittivity increment $\Delta\varepsilon'(\omega, \phi)$ from the cell model normalized with $\phi\varepsilon_s$ exhibits a rapid decrease with increasing volume fraction. This arises from two contributions. First the double layer polarizability (which depends on the equilibrium double layer charge density and hence follows $\sigma^{(0)}(\phi)$) will decrease with ϕ. Second, the effect of replacing highly polarizable solvent (in these calculations, water) with low permittivity solid, decreases the effective polarizability faster than the linear decrease with ϕ expected at low volume fractions. At the larger κa value ($\kappa a = 5$) the double layer polarizability reflects the larger $\sigma^{(0)}(\phi)$ and accordingly, $\Delta\varepsilon'(\omega, \phi)/(\phi\varepsilon_s)$ (Figure 8b) is correspondingly larger than the $\kappa a = 1$ case (Figure 5b).

At the very high frequency 10^8 Hz, the normalized conductivity decreases slightly with volume fraction—the effect being more pronounced at higher zeta values. This is presumably due to the interference of the impenetrable particle with the ion trajectories which decrease as the amplitude of ion oscillation decreases with frequency. The intermediate frequency case at 10^5 Hz shows behavior between these two extremes with the ion excess effect dominating at lower ϕ and the trajectory effect at higher ϕ. The dielectric permittivity at high frequency (Figures 7b for $\kappa a = 1$ and 10b for $\kappa a = 5$) shows a striking *independence* of the zeta potential. This may be understood from Figure 11, where we see that the ion diffusion length and the hydrodynamic penetration depth are restricted to a boundary layer close to the particle surface for the 10^8 Hz case. The physical implications of this boundary layer have been discussed in detail for the isolated particle case by Ennis and White[16] and more recently by Hill et al.[39]

A boundary layer analysis[40] in the spirit of Ennis and White[16] reveals that to order ω^{-1},

$$\Delta\varepsilon' = \frac{3\varepsilon_s\phi(1-\varepsilon_p/\varepsilon_s)}{2+\phi+(1-\phi)\varepsilon_p/\varepsilon_s} \tag{14}$$

independent of ζ and κa, and this equation describes the data in Figures 7b and 10b well.

The dielectric response of a dense suspension of charged spherical particles to an applied electric field is readily accessible by our cell-model theory of electrokinetics[1−3] accounting in a mean field way for both static and dynamic particle−particle interactions over the entire volume fraction range. The model's predictions of complex conductivity compare favorably with published experimental measurements on dense colloidal systems. There are, however, some systems (e.g., dispersions of particles with nonideal polymeric surfaces) where the prediction of complex permittivity with this model is not accurate. It is likely that permittivity calculations on these systems can be improved by the inclusion of effects such as surface conduction and polymeric drag.

Acknowledgment. The authors wish to thank the referees for useful comments on an earlier version of this paper.

LA8028963

(39) Hill, R. J.; Saville, D. A.; Russel, W. B. *Phys. Chem. Chem. Phys.* **2003**, *5*, 911.
(40) Bradshaw-Hajek, B. H.; Miklavcic, S. J.; White, L. R., in preparation.